Radiative corrections to elastic proton-electron scattering measured in coincidence

G. I. Gakh, M. I. Konchatnij, and N. P. Merenkov
NSC "Kharkov Institute of Physics and Technology," Akademicheskaya, 1, 61108 Kharkov, and V.N. Karazin Kharkiv National University, 61022 Kharkov, Ukraine

E. Tomasi-Gustafsson
IRFU, CEA, Université Paris-Saclay, 91191 Gif-sur-Yvette Cedex, France

(Received 4 December 2016; revised manuscript received 2 March 2017; published 30 May 2017)

The differential cross section for elastic scattering of protons on electrons at rest is calculated, taking into account the QED radiative corrections to the leptonic part of interaction. These model-independent radiative corrections arise due to emission of the virtual and real soft and hard photons as well as to vacuum polarization. We analyze an experimental setup when both the final particles are recorded in coincidence and their energies are determined within some uncertainties. The kinematics, the cross section, and the radiative corrections are calculated and numerical results are presented.

DOI: 10.1103/PhysRevC.95.055207

I. INTRODUCTION

The polarized and unpolarized scattering of electrons off protons has been widely studied, as it is considered the simpler way to access information on the proton structure, assuming that the interaction occurs through the exchange of a virtual photon of four-momentum q. The experimental determination of the elastic proton electromagnetic form factors in the region of small and large momentum transfer squared is one of the major field of research in hadron physics (see the review in Ref. [1]). New experimental possibilities have allowed us to reach better precision and to perform polarization experiments as earlier suggested in Refs. [2,3].

The determination of the proton electromagnetic form factors, at $Q^2 = -q^2 \geqslant 1$ GeV^2, from polarization observables showed a surprising result: the polarized and unpolarized experiments, although based on the same theoretical background (same formalism and same assumptions), ended up with inconsistent values of the form factor ratio (see Ref. [4] and references therein). A possible explanation of this discrepancy is to take into account higher-order radiative corrections [5,6] including the interference between one- and two-photon exchange [7], correlations among parameters [8], and normalization of data [9]. This puzzle has given rise to many speculations and different interpretations, suggesting further experiments (for a review, see Ref. [10]).

In the region of small Q^2 one can determine the proton charge radius (r_E), which is one of the fundamental quantities in physics. Precise knowledge of its value is important for the understanding of the structure of the nucleon in the theory of strong interactions (QCD) as well as in the spectroscopy of atomic hydrogen.

Recently, the determination of the r_E with muonic atoms lead to the so-called proton radius puzzle. Experiments on muonic hydrogen by laser spectroscopy measurement of the μp $(2S-2P)$ transition frequency, in particular the latest result on the proton charge radius [11,12] $r_E = 0.84087(39)$ fm, is one order of magnitude more precise but smaller by seven standard deviations compared to the average value $r_E = 0.8775(51)$ fm, which is recommended by the 2010-CODATA review [13]. The CODATA value is obtained coherently from hydrogen atom spectroscopy and electron-proton elastic scattering measurements. The latest experiments with electrons at Jlab [14] and MAMI [15] confirm this value, and, therefore, do not agree with the results on the proton radius from the laser spectroscopy of the muonic hydrogen.

While the corrections to the laser spectroscopy experiments seem well under control in the frame of QED and may be estimated with a precision better than 0.1%, in the case of electron-proton elastic scattering the best achieved precision is of the order of few percentages. Different sources of possible systematic errors of the muonic experiment have been discussed; however, no definite explanation of this difference has been given yet (see Ref. [16] and references therein).

The proton radius puzzle lead to a large number of theoretical papers suggesting solutions based on different approaches, as new physics beyond the Standard Model [17,18]. Other approaches analyze the extraction of the proton radius from the electron-proton scattering data. In Ref. [19], it is argued that a proper Lorentz transformation of the form factors accounts for the discrepancy. The authors of Ref. [20] stated that radius extraction with Taylor series expansions cannot be trusted to be reliable. A fit function based on a conformal mapping was used in Refs. [21,22]. The extracted value of the proton radius agrees with the one obtained from muonic hydrogen. A similar result was obtained in Ref. [23] using the approach based on the chiral perturbation theory [24].

In Ref. [25], the authors argued that the proton radius puzzle can be explained by truncating the electron scattering data to low momentum transfer. But the authors of Ref. [26] showed that the procedure is inconsistent and violates the Fourier theorem. The authors of the paper [27] inspected several recent refits of the Mainz data that result in small radii and found flaws of various kinds in all of them.

A recent review summarizes the current state of the problem and gives an overview over upcoming experiments [28].

More experiments in the region of small Q^2 are expected to shed some light on this intriguing problem. The PRad collaboration [29] is currently preparing a new magnetic-spectrometer-free electron-proton scattering experiment in

Hall B at the Jefferson Lab for a new independent measurement of r_E. This will allow us to reach an extremely low Q^2 range $(10^{-4}$–$10^{-2})\,(\mathrm{GeV}/c)^2$ with an incident electron beams with energy of few GeV. The lowest Q^2 range measured until now is in the recent Mainz experiment [15] where the minimum value of Q^2 was $3\times10^{-3}\,(\mathrm{GeV}/c)^2$. Reaching a low Q^2 range is critically important since the charge radius of the proton is extracted as the slope of the measured electric form factor $G_p^E(Q^2)$ for $Q^2\to 0$, requiring an extrapolation. The MUSE experiment [30] (PSI, Switzerland) will simultaneously measure elastic electron and muon scattering on the proton in both charge states. The expected precision on cross-section measurements for the elastic scattering of $\mu^{+/-}$ and $e^{+/-}$ is better than the percentage over a Q^2 range from 0.002 to 0.07 GeV^2. Low-energy ep scattering experiments are also planned at the PRAE platform [31], making use of a high-intensity low-energy electron beam and with a very precise measurement of the electron angle and energy. At the Mainz Microtron, the simultaneous detection of the proton and the electron is proposed [32] in the measurement of the absolute cross section at per-mille absolute precision.

Recently, we suggested that proton elastic scattering on atomic electrons may allow a precise measurement of the proton charge radius [33]. The main advantage of this proposal is that inverse kinematics allows one to access very small values of the transferred momenta, up to four orders of magnitude smaller than the ones presently achieved, where the cross section is huge. Moreover, the applied radiative corrections differ essentially, as the electron mass should be taken explicitly into account. The unpolarized and polarized observables for the elastic scattering of a proton projectile on an electron target were derived in Ref. [34] and references therein. Although we are aware that an experiment measuring the elastic cross section at very small Q^2 cannot, by itself, produce a constraint on the slope of form factors, and therefore a precise extraction of the radius, a combined series of low Q^2 very precise measurements, combined with a physical parametrization of form factors, will help for a meaningful extrapolation to the static point.

The inverse kinematics was previously used in a number of the experiments to measure the pion or kaon radius from the elastic scattering of negative pions (kaons) from electrons in a liquid-hydrogen target. The first experiment was done at Serpukhov [35] with pion beam energy of 50 GeV. Later, a few experiments were done at Fermilab with a pion beam energy of 100 GeV [36] and 250 GeV [37]. At this laboratory, the electromagnetic form factors of negative kaons were measured by direct scattering of 250 GeV kaons on stationary electrons [38]. The typical values of the radiative corrections in this case are of the order of 7–10% [39,40]. Later, a measurement of the pion electromagnetic form factor was done at the CERN SPS [41,42] by measuring the interaction of 300 GeV pions with the electrons in a liquid hydrogen target. This experiment measured only the angles of the final particles to select the pion-electron elastic events, whereas, in previous experiments, both three-momenta were measured.

The use of the inverse kinematics is proposed in a new experiment at CERN [43] to measure the running of the fine-structure constant in the spacelike region by scattering high-energy muons (with energy 150 GeV) on atomic electrons, $\mu e\to\mu e$. The aim of the experiment is the extraction of the hadron vacuum polarization contribution. The proposed technique will be similar to the one described in Refs. [41,42] for the measurement of the pion form factor: a precise measurement of the scattering angles of both outgoing particles.

For the analysis of the results of the possible experiment on the elastic proton-electron scattering, it is necessary to take into account radiative corrections. In this paper we calculate the model-independent QED radiative corrections to the differential cross section of the elastic scattering of the protons on electrons at rest. The radiative corrections due to the emission of virtual and real (soft and hard) photons in the electron vertex as well the vacuum polarization are taken into account. The corresponding Feynmann diagrams are shown in Fig. 1. We consider an experimental setup where the final particles are detected in coincidence and their energies are measured within some uncertainty. Numerical estimations of

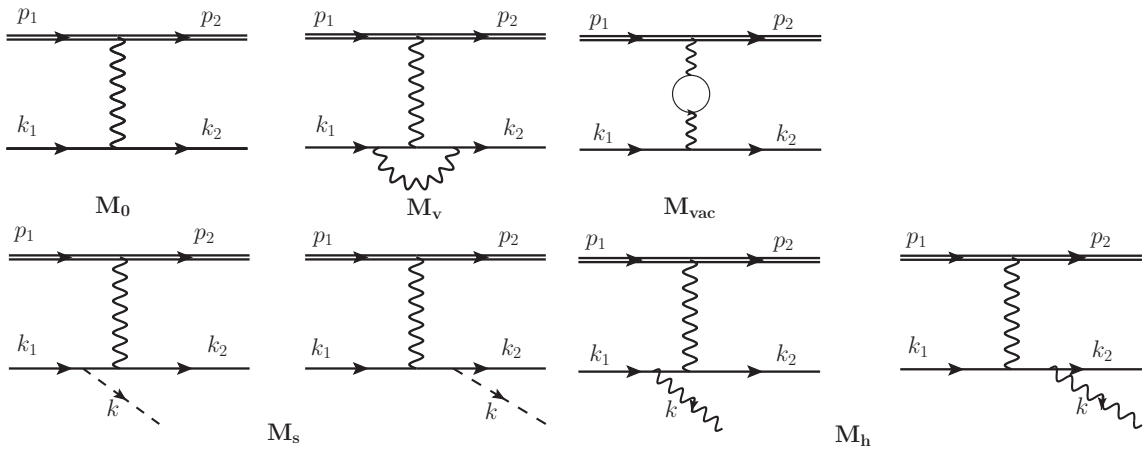

FIG. 1. Feynman's diagrams corresponding to the Born approximation and first-order virtual radiative corrections (top), and to initial and final real photon emission, M_s (soft) and M_h (hard), from the lepton vertex (bottom).

these corrections in the considered case are given and their dependence on the kinematical variables is illustrated.

II. FORMALISM

Let us consider the reaction

$$p(p_1) + e(k_1) \rightarrow p(p_2) + e(k_2), \tag{1}$$

where the particle momenta are indicated in parenthesis and $q = k_1 - k_2 = p_2 - p_1$ is the four-momentum of the virtual photon.

A. Inverse kinematics

A general characteristic of all reactions of elastic and inelastic hadron scattering by atomic electrons (which can be considered at rest) is the small value of the momentum transfer squared, even for relatively large energies of the colliding particles. Let us give details of the order of magnitude and the dependence of the kinematic variables, as they are very specific for these reactions. In particular, the electron mass cannot be neglected in the kinematics and dynamics of the reaction, even when the beam energy is of the order of GeV.

One can show that, for a given energy of the proton beam, the maximum value of the four-momentum transfer squared, in the scattering on electrons at rest, is

$$(Q^2)_{\max} = \frac{4m^2\vec{p}^2}{M^2 + 2mE + m^2}, \tag{2}$$

where $m(M)$ is the electron (proton) mass and $E(\vec{p})$ is the energy (momentum) of the proton beam. Being proportional to the electron mass squared, the four-momentum transfer squared is restricted to very small values, where the proton can be considered structureless.

The four-momentum transfer squared is expressed as a function of the energy of the scattered electron, ϵ_2, as $q^2 = (k_1 - k_2)^2 = 2m(m - \epsilon_2)$, where

$$\epsilon_2 = m\frac{(E+m)^2 + \vec{p}^2\cos^2\theta_e}{(E+m)^2 - \vec{p}^2\cos^2\theta_e}, \tag{3}$$

where θ_e is the angle between the proton beam and the scattered electron momenta.

From energy and momentum conservation, one finds the following relation between the angle and the energy of the scattered electron:

$$\cos\theta_e = \frac{(E+m)(\epsilon_2 - m)}{|\vec{p}|\sqrt{\epsilon_2^2 - m^2}}, \tag{4}$$

which shows that $\cos\theta_e \geqslant 0$ (the electron can never be scattered backward). One can see from Eq. (3) that, in inverse kinematics, the available kinematical region is reduced to small values of ϵ_2:

$$\epsilon_{2,\max} = m\frac{2E(E+m) + m^2 - M^2}{M^2 + 2mE + m^2}, \tag{5}$$

which is proportional to the electron mass. From the momentum conservation, one can find the following relation between the energy and the angle of the scattered proton E_2 and θ_p:

$$E_2^{\pm} = \frac{(E+m)(M^2+mE) \pm M\vec{p}^2\cos\theta_p\sqrt{\frac{m^2}{M^2} - \sin^2\theta_p}}{(E+m)^2 - \vec{p}^2\cos^2\theta_p}, \tag{6}$$

showing that, for one proton angle, there may be two values of the proton energies (and two corresponding values for the recoil-electron energy and angle as well as for the transferred momentum q^2). This is a typical situation when the center-of-mass velocity is larger than the velocity of the projectile in the center of mass, where all the angles are allowed for the recoil electron. The two solutions coincide when the angle between the initial and final hadron takes its maximum value, which is determined by the ratio of the electron and scattered hadron masses M_h, $\sin\theta_{h,\max} = m/M_h$. One concludes that hadrons are scattered on atomic electrons at very small angles and that the larger the hadron mass, the smaller the available angular range for the scattered hadron.

B. Differential cross section

In the one-photon exchange (Born) approximation, the matrix element $\mathcal{M}^{(B)}$ of the reaction (1) can be written as

$$\mathcal{M}^{(B)} = \frac{e^2}{q^2} j_\mu J_\mu, \tag{7}$$

where $j_\mu(J_\mu)$ is the leptonic (hadronic) electromagnetic current:

$$\begin{aligned} j_\mu &= \bar{u}(k_2)\gamma_\mu u(k_1), \\ J_\mu &= \bar{u}(p_2)\left[F_1(q^2)\gamma_\mu - \frac{1}{2M}F_2(q^2)\sigma_{\mu\nu}q_\nu\right]u(p_1) \\ &= \bar{u}(p_2)\left[G_M(q^2)\gamma_\mu - F_2(q^2)P_\mu\right]u(p_1), \end{aligned} \tag{8}$$

where $P_\mu = (p_1 + p_2)_\mu/(2M)$. $F_1(q^2)$ and $F_2(q^2)$ are the Dirac and Pauli proton electromagnetic form factors, and $G_M(q^2) = F_1(q^2) + F_2(q^2)$ is the Sachs proton magnetic form factor. The matrix element squared is written as

$$|\mathcal{M}^{(B)}|^2 = 16\pi^2\frac{\alpha^2}{q^4}L_{\mu\nu}W_{\mu\nu}, \text{ with } L_{\mu\nu} = j_\mu j_\nu^*, W_{\mu\nu} = J_\mu J_\nu^*, \tag{9}$$

where $\alpha = e^2/(4\pi) = 1/137$ is the electromagnetic fine structure constant. The leptonic tensor, $L_{\mu\nu}$, for unpolarized initial and final electrons (averaging over the initial electron spin) has the form:

$$L_{\mu\nu} = q^2 g_{\mu\nu} + 2(k_{1\mu}k_{2\nu} + k_{1\nu}k_{2\mu}). \tag{10}$$

The hadronic tensor $W_{\mu\nu}$, for unpolarized initial and final protons can be written in the standard form, through two unpolarized structure functions:

$$W_{\mu\nu} = \left(-g_{\mu\nu} + \frac{q_\mu q_\nu}{q^2}\right)W_1(q^2) + P_\mu P_\nu W_2(q^2). \tag{11}$$

Averaging over the initial proton spin, the structure functions $W_i, i = 1,2$, are expressed in terms of the nucleon electromag-

netic form factors:

$$W_1(q^2) = -q^2 G_M^2(q^2),\ W_2(q^2) = 4M^2 \frac{G_E^2(q^2) + \tau G_M^2(q^2)}{1+\tau}, \tag{12}$$

where $G_E(q^2) = F_1(q^2) - \tau F_2(q^2)$ is the proton electric form factor and $\tau = -q^2/4M^2$.

The expression of the differential cross section, as a function of the recoil-electron energy ϵ_2, for unpolarized proton-electron scattering can be written as

$$\frac{d\sigma^{(B)}}{d\epsilon_2} = \frac{\pi\alpha^2}{m\vec{p}^2}\frac{\mathcal{D}}{q^4}, \tag{13}$$

with

$$\mathcal{D} = q^2(q^2+2m^2)G_M^2(q^2) + 2\left[q^2M^2 + \frac{1}{1+\tau}\left(2mE + \frac{q^2}{2}\right)^2\right] \times \left[G_E^2(q^2) + \tau G_M^2(q^2)\right]. \tag{14}$$

This expression is valid in the one-photon exchange (Born) approximation in the reference system where the target electron is at rest.

The expression of the differential cross section, as a function of the four-momentum transfer squared, is

$$\frac{d\sigma^{(B)}}{dq^2} = \frac{\pi\alpha^2}{2m^2\vec{p}^2}\frac{\mathcal{D}}{q^4}. \tag{15}$$

Last, the differential cross section over the scattered-electron solid angle has the following expression:

$$\frac{d\sigma^{(B)}}{d\Omega_e} = \frac{\alpha^2}{8m^4|\vec{p}|}\left(1 - \frac{4m^2}{q^2}\right)^{3/2}\frac{\mathcal{D}}{E+m}. \tag{16}$$

III. RADIATIVE CORRECTIONS

Let us consider the model-independent QED radiative corrections which are due to the vacuum polarization and emission of the virtual and real (soft and hard) photons in the electron vertex. The corresponding diagrams are shown in Fig. 1.

A. Soft photon emission

In this section we calculate the contribution to the radiative corrections of the soft photon emission when the photons are emitted by the initial and final electrons,

$$p(p_1) + e(k_1) \to p(p_2) + e(k_2) + \gamma(k). \tag{17}$$

The matrix element in this case (the photon emitted from the electron vertex) is given by

$$\mathcal{M}^{(\gamma)} = \frac{1}{q^2}(4\pi\alpha)^{3/2} j_\mu^{(\gamma)} J_\mu, \tag{18}$$

where the electron current corresponding to the photon emission is

$$j_\mu^{(\gamma)} = \bar{u}(k_2)\left[\frac{1}{d_1}\gamma_\mu(\hat{k}_1 - \hat{k} + m)\gamma_\rho + \frac{1}{d_2}\gamma_\rho(\hat{k}_2 + \hat{k} + m)\gamma_\mu\right] \times u(k_1)A_\rho^*, \tag{19}$$

where A_ρ is the polarization vector of the emitted photon and $d_1 = -2k\cdot k_1, d_2 = 2k\cdot k_2$.

The differential cross section of reaction (17) can be written as

$$d\sigma^{(\gamma)} = \frac{(2\pi)^{-5}}{32m|\vec{p}|}|\mathcal{M}^{(\gamma)}|^2 \frac{d^3\vec{k}_2}{\epsilon_2}\frac{d^3\vec{p}_2}{E_2}\frac{d^3\vec{k}}{\omega} \times \delta^4(k_1 + p_1 - k_2 - p_2 - k). \tag{20}$$

It is necessary to integrate over the photon phase space. Since the photons are assumed to be soft, then the integration over the photon energy is restricted to $\omega \leqslant \bar{\omega}$. The quantity $\bar{\omega}$ is determined by particular experimental conditions and it is assumed that $\bar{\omega}$ is sufficiently small to neglect the momentum k in the δ function and in the numerators of the matrix element $\mathcal{M}^{(\gamma)}$. In order to avoid the infrared divergence, which occurs in the soft photon cross section, a small fictitious photon mass λ is introduced.

In the soft photon approximation, the matrix element (18) is

$$\mathcal{M}^{(\text{soft})} = \sqrt{4\pi\alpha}\left(\frac{k_2\cdot A^*}{k\cdot k_2} - \frac{k_1\cdot A^*}{k\cdot k_1}\right)\mathcal{M}^{(B)}. \tag{21}$$

The differential cross section (20), integrated over the soft photon phase space, can be written as

$$d\sigma^{(\text{soft})} = \delta^{(s)} d\sigma^{(B)}, \tag{22}$$

where the radiative correction due to the soft photon emission is

$$\delta^{(s)} = -\frac{\alpha}{4\pi^2}\int_\lambda^{\bar{\omega}}\sqrt{\omega^2-\lambda^2}d\omega\int d\Omega_k \times \left[\frac{m^2}{(k\cdot k_1)^2} + \frac{m^2}{(k\cdot k_2)^2} - 2\frac{k_1\cdot k_2}{k\cdot k_1 k\cdot k_1}\right]. \tag{23}$$

Assuming $\bar{\omega} \ll m$ and using the results of the paper [44], we can do the integration and the expression for $\delta^{(s)}$ has the form

$$\delta^{(s)} = \frac{\alpha}{\pi}\left\{1 - 2\ln\frac{2\bar{\omega}}{\lambda} + \frac{\epsilon_2}{k_2}\left[\ln\frac{\epsilon_2+k_2}{m} \times \left(1 + 2\ln\frac{2\bar{\omega}}{\lambda} + \ln\frac{\epsilon_2+k_2}{m} + 2\ln\frac{m}{2k_2}\right) - \frac{\pi^2}{6} + Li_2\left(\frac{\epsilon_2-k_2}{\epsilon_2+k_2}\right)\right]\right\}, \tag{24}$$

where $k_2 \equiv |\vec{k}_2|$ ($\vec{k}_2$ is the momentum of the recoil electron) and $Li_2(x)$ is the Spence (dilogarithm) function defined as

$$Li_2(x) = -\int_0^x \frac{\ln(1-t)}{t}dt.$$

B. Virtual photon emission

In this section, we calculate the contribution to the radiative corrections of the virtual photon emission in the electron vertex (the electron vertex correction) and the vacuum polarization term.

The matrix element corresponding to this process can be written as

$$\mathcal{M}^{(\mathrm{virt})} = \frac{1}{q^2} 4\pi\alpha J_\mu \bar{u}(k_2)\Lambda_\mu(k_1,k_2)u(k_1), \tag{25}$$

where we introduce

$$\Lambda_\mu(k_1,k_2) = \frac{2i\alpha}{(2\pi)^3}\int \frac{d^4k}{k^2-\lambda^2}\frac{\hat{O}_\mu}{(k^2-2k\cdot k_1)(k^2-2k\cdot k_2)} \tag{26}$$

and the matrix $\hat{O}_\mu$ is

$$\hat{O}_\mu = 4k_1\cdot k_2\gamma_\mu - 2(\hat{k}_1\hat{k}\gamma_\mu + \gamma_\mu\hat{k}\hat{k}_2) - 2\hat{k}\gamma_\mu\hat{k}. \tag{27}$$

The integration over the virtual-photon four-momentum k leads to the following expression for the function $\Lambda_\mu(k_1,k_2)$:

$$\Lambda_\mu(k_1,k_2) = \frac{\alpha}{4\pi}\left(\left\{\ln\frac{\Lambda^2}{m^2} + \frac{1}{2} + \int_0^1 \frac{dx}{P_x^2}\left[4m^2 - \frac{3}{2}q^2 + (q^2-2m^2)\left(\ln\frac{P_x^2}{m^2} + \ln\frac{m^2}{\lambda^2}\right)\right]\right\}\gamma_\mu + m\int_0^1 \frac{dx}{P_x^2}\sigma_{\mu\nu}q_\nu\right), \tag{28}$$

where $P_x^2 = m^2 - x(1-x)q^2$ and Λ is the cut parameter which defines the region of infinite momenta of the virtual photon. Thus we avoid the ultraviolet divergence. The regularized vertex function can be obtained subtracting the contribution

$$\Lambda_\mu(k_1,k_1) = \frac{\alpha}{4\pi}\gamma_\mu\left(\ln\frac{\Lambda^2}{m^2} + \frac{9}{2} - 2\ln\frac{m^2}{\lambda^2}\right)$$

from the expression (28). As a result, we have

$$\Lambda_\mu^R(k_1,k_2) = \Lambda_\mu(k_1,k_2) - \Lambda_\mu(k_1,k_1) = \frac{\alpha}{4\pi}(A\gamma_\mu + B\sigma_{\mu\nu}q_\nu), \tag{29}$$

where

$$A = -4 + 2\ln\frac{m^2}{\lambda^2} + \int_0^1 \frac{dx}{P_x^2}\left[4m^2 - \frac{3}{2}q^2 + (q^2-2m^2)\left(\ln\frac{P_x^2}{m^2} + \ln\frac{m^2}{\lambda^2}\right)\right],\quad B = m\int_0^1 \frac{dx}{P_x^2}. \tag{30}$$

As we limit ourselves to the calculation of the radiative corrections at the order of α in comparison with the Born term, it is sufficient to calculate the interference of the Born matrix element with $\mathcal{M}^{(\mathrm{virt})}$,

$$|\mathcal{M}|^2 = |\mathcal{M}^{(B)}|^2 + 2Re[\mathcal{M}^{(\mathrm{virt})}\mathcal{M}^{(B)*}] = (1+\delta_1+\delta_2)|\mathcal{M}^{(B)}|^2, \tag{31}$$

where the term δ_1 is due to the modification of the γ_μ term in the electron vertex, and the term δ_2 is due to the presence of the $\sigma_{\mu\nu}q_\nu$ structure in the electron vertex.

The integration over the x variable in the expression (30) gives the following results for the radiative corrections due to the emission of the virtual photon in the electron vertex

$$\begin{aligned}\delta_1 = \frac{\alpha}{\pi}\Bigg(&-2 + 2\ln\frac{m}{\lambda}\left[1 - \frac{\epsilon_2}{k_2}\ln\left(\frac{\epsilon_2+k_2}{m}\right)\right] + \frac{m+3\epsilon_2}{2k_2}\ln\left(\frac{\epsilon_2+k_2}{m}\right) - \frac{1}{2}\frac{\epsilon_2}{k_2}\ln\left(\frac{Q^2}{m^2}\right)\ln\left(\frac{\epsilon_2+k_2}{m}\right)\\ &+\frac{\epsilon_2}{k_2}\left\{-\ln\left(\frac{m+\epsilon_2}{k_2}\right)\ln\left(\frac{\epsilon_2+k_2}{m}\right) + Li_2\left[\frac{\epsilon_2+k_2+m}{2(m+\epsilon_2)}\right] - Li_2\left[\frac{\epsilon_2-k_2+m}{2(m+\epsilon_2)}\right\}\right]\Bigg),\\ \delta_2 = 4\frac{\alpha}{\pi}\frac{mM^2q^2}{k_2\mathcal{D}}&\ln\left(\frac{\epsilon_2+k_2}{m}\right)(G_E^2 - 2\tau G_M^2).\end{aligned} \tag{32}$$

The radiative correction due to the vacuum polarization is (the electron loop has been taken into account):

$$\delta^{(\mathrm{vac})} = \frac{2\alpha}{3\pi}\left\{-\frac{5}{3} + 4\frac{m^2}{Q^2} + \left(1-2\frac{m^2}{Q^2}\right)\sqrt{1+4\frac{m^2}{Q^2}}\ln\frac{\sqrt{1+4\frac{m^2}{Q^2}}+1}{\sqrt{1+4\frac{m^2}{Q^2}}-1}\right\}. \tag{33}$$

For small and large values of the Q^2 variable, we have

$$\text{If}\quad Q^2 \ll m^2,\quad \delta^{(\mathrm{vac})} = \frac{2\alpha}{15\pi}\frac{Q^2}{m^2},\quad \text{If}\quad Q^2 \gg m^2,\quad \delta^{(\mathrm{vac})} = \frac{2\alpha}{3\pi}\left(-\frac{5}{3} + \ln\frac{Q^2}{m^2}\right).$$

Taking into account the radiative corrections given by Eqs. (24), (32), and (33), we obtain the following expression for the differential cross section:

$$d\sigma^{(\mathrm{RC})} = [1+\delta_1+\delta_2+\delta^{(s)}+\delta^{(\mathrm{vac})}]d\sigma^{(B)} = [1+\delta_0+\bar{\delta}+\delta^{(\mathrm{vac})}]d\sigma^{(B)}, \tag{34}$$

where the radiative corrections δ_0 and $\bar{\delta}$ are given by

$$\delta_0 = \frac{2\alpha}{\pi}\ln\frac{\bar{\omega}}{m}\left[\frac{\epsilon_2}{k_2}\ln\left(\frac{\epsilon_2+k_2}{m}\right)-1\right],$$

$$\bar{\delta} = \frac{\alpha}{\pi}\left(-1-2\ln 2+\frac{\epsilon_2}{k_2}\left\{\ln\left(\frac{\epsilon_2+k_2}{m}\right)\left[1+\ln\left(\frac{\epsilon_2+k_2}{m}\right)+2\ln\left(\frac{m}{k_2}\right)+\frac{m+3\epsilon_2}{2\epsilon_2}-\ln\left(\frac{\epsilon_2+m}{k_2}\right)-\frac{1}{2}\ln\left(\frac{Q^2}{m^2}\right)\right]\right.$$
$$\left.+4m\frac{M^2q^2}{\epsilon_2\mathcal{D}}\ln\left(\frac{\epsilon_2+k_2}{m}\right)(G_E^2-2\tau G_M^2)-\frac{\pi^2}{6}+Li_2\left(\frac{\epsilon_2-k_2}{\epsilon_2+k_2}\right)+Li_2\left[\frac{\epsilon_2+k_2+m}{2(\epsilon_2+m)}\right]-Li_2\left[\frac{\epsilon_2-k_2+m}{2(\epsilon_2+m)}\right]\right\}\right). \quad (35)$$

We separate the contribution δ_0 since it can be summed up in all orders of the perturbation theory using the exponential form of the electron structure functions [45]. To do this it is sufficient to keep only the exponential contributions in the electron structure functions. The final result can be obtained by the substitution of the term $(1+\delta_0)$ by the following term:

$$\left(\frac{\bar{\omega}}{m}\right)^{\beta}\frac{\beta}{2}\int_0^1 x^{\frac{\beta}{2}-1}(1-x)^{\frac{\beta}{2}}dx, \quad (36)$$

where

$$\beta = \frac{2\alpha}{\pi}\left[\frac{\epsilon_2}{k_2}\ln\left(\frac{\epsilon_2+k_2}{m}\right)-1\right].$$

C. Hard photon emission

In this section we calculate the radiative correction due to the hard photon emission by the initial and recoil electrons only (the model-independent part). The contribution due to radiation from the initial and scattered protons (the model-dependent part) requires a special consideration and we leave it for other investigations. We consider the experimental setup when only the energies of the scattered proton and final electron are measured.

The differential cross section of the reaction (17), averaged over the initial particle spins, can be written as

$$d\sigma^{(h)} = \frac{\alpha^3}{32\pi^2}\frac{1}{m\,p}\frac{L_{\mu\nu}^{(\gamma)}W_{\mu\nu}}{q_1^4}\frac{d^3k_2}{\epsilon_2}\frac{d^3p_2}{E_2}\frac{d^3k}{\omega}\delta^4(p_1+k_1-p_2-k_2-k), \quad (37)$$

where $q_1 = k_1-k_2-k$ and the leptonic tensor has the following form:

$$L_{\mu\nu}^{(\gamma)} = A_0\tilde{g}_{\mu\nu}+A_1\tilde{k}_{1\mu}\tilde{k}_{1\nu}+A_2\tilde{k}_{2\mu}\tilde{k}_{2\nu}+A_{12}(\tilde{k}_{1\mu}\tilde{k}_{2\nu}+\tilde{k}_{1\nu}\tilde{k}_{2\mu}),$$
$$A_0 = 4\left[\frac{d_1}{d_2}+\frac{d_2}{d_1}-2q_1^2\left(\frac{m^2}{d_1^2}+\frac{m^2}{d_2^2}+2\frac{k_1\cdot k_2}{d_1d_2}\right)\right],\ A_1 = 16\frac{q_1^2}{d_1d_2}-32\frac{m^2}{d_2^2},$$
$$A_2 = 16\frac{q_1^2}{d_1d_2}-32\frac{m^2}{d_1^2},\ A_{12} = -32\frac{m^2}{d_1d_2}. \quad (38)$$

The hadronic tensor is defined by Eqs. (11) and (12) with the substitution $q\to q_1$.

The contraction of leptonic and hadronic tensors reads

$$L_{\mu\nu}^{(\gamma)}W_{\mu\nu} = -W_1(q_1^2)\,S_1+\frac{W_2(q_1^2)}{M^2}\,S_2, \quad (39)$$

where the functions $S_{1,2}$ have the following expressions:

$$S_1 = 8\left(\frac{d_1}{d_2}+\frac{d_2}{d_1}\right)-\frac{16}{d_1d_2}(2m^2+q_1^2)\left[2k_1\cdot k_2+m^2\left(\frac{d_1}{d_2}+\frac{d_2}{d_1}\right)\right], \quad (40)$$

$$S_2 = 4M^2\left[\frac{d_1}{d_2}+\frac{d_2}{d_1}-2q_1^2\left(\frac{m^2}{d_1^2}+\frac{m^2}{d_2^2}+2\frac{k_1\cdot k_2}{d_1d_2}\right)\right]+32\frac{m^2}{d_1d_2}(k\cdot p_1)^2+16\frac{(k_1\cdot p_1)^2}{d_1}+16\frac{(k_2\cdot p_1)^2}{d_2}+16k_1\cdot p_1k_2\cdot p_1$$
$$\times\left[\frac{1}{d_1}+\frac{1}{d_2}-2\left(\frac{m^2}{d_1^2}+\frac{m^2}{d_2^2}+2\frac{k_1\cdot k_2}{d_1d_2}\right)\right]$$
$$+16k\cdot p_1\left[\frac{k_1\cdot p_1}{d_2^2}(d_2-2m^2)-\frac{k_2\cdot p_1}{d_1^2}(d_1-2m^2)+2\frac{k_1\cdot k_2}{d_1d_2}(k_2\cdot p_1-k_1\cdot p_1)\right]. \quad (41)$$

Integrating over the scattered proton variables we obtain the following expression for the differential cross section:

$$d\sigma^{(h)} = \frac{\alpha^3}{32\pi^2}\frac{1}{mp}\int\frac{d^3k}{\omega}\int\frac{d^3k_2}{\epsilon_2\,E_2}\frac{1}{q_1^4}L_{\mu\nu}^{(\gamma)}W_{\mu\nu}\,\delta(m+E-\epsilon_2-E_2-\omega). \quad (42)$$

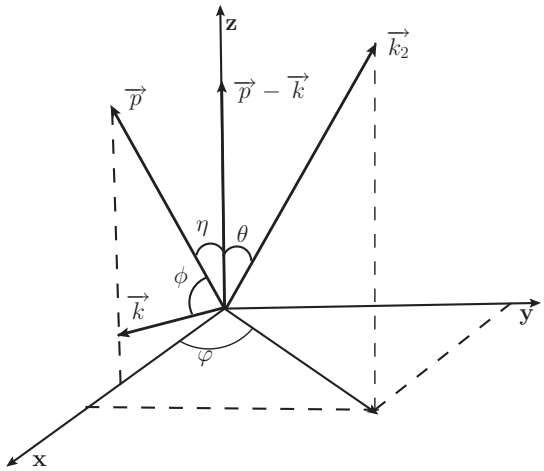

FIG. 2. Coordinate system and definition of the angles used for the integration over the variables of the final state.

To integrate further we have to define the coordinate system. Following Ref. [39], where the $\pi - e^-$ scattering has been analyzed, let us take the z axis along the vector $\vec{p} - \vec{k}$ and the momenta of the initial proton and emitted photon lie in the xz plane. The momentum of the scattered electron is defined by the polar θ and azimuthal φ angles as it is shown in Fig. 2. The angle $\eta(\phi)$ is the angle between the beam direction and z axis (emitted photon momentum).

Integrating over the polar angle of the scattered electron we obtain:

$$\frac{d\sigma^{(h)}}{d\epsilon_2} = \frac{\alpha^3}{32\pi^2}\frac{1}{mp}\int\frac{d^3k}{\omega}\int\frac{d\varphi}{|\vec{p}-\vec{k}|}\frac{1}{q_1^4}L^{(\gamma)}_{\mu\nu}W_{\mu\nu}. \quad (43)$$

The region of allowed photon momenta should be determined. The experiment counts those events which, within the accuracy of the detectors, are considered "elastic." We refer to the experimental situation where the energies of the scatted proton and recoil electron are measured. Because of the uncertainties in determination of the recoil electron ($\Delta\epsilon_2$) and scattered proton (ΔE_2) energies, which usually are proportional to ϵ_2 and E_2, respectively, the elastic proton-electron is always accompanied by hard photon emission with energies up to $\Delta\epsilon_2 + \Delta E_2$. At the proton beam energies of the order of 100 GeV this value can reach a few GeV. The events for which the scattered proton energy is $E_2 \pm \Delta E_2$ and the recoil electron energy is $\epsilon_2 \pm \Delta\epsilon_2$ (they satisfy the condition $E + m = E_2 + \epsilon_2$) are considered as true elastic events. Here, ΔE_2 and $\Delta\epsilon_2$ are the errors in the measurement of the final proton and recoil electron energies. The plot of the variable E_2 versus the variable ϵ_2 is shown in Fig. 3. The shaded area in this figure represents those events allowed by the experimental limitations. The relation between the energies E_2 and ϵ_2, as it is shown in Fig. 3, has to be transformed into a limit on the possible photon momentum $\vec{k}$. We consider the experimental setup where no angles are measured and, therefore, the orientation of the photon momentum $\vec{k}$ is not

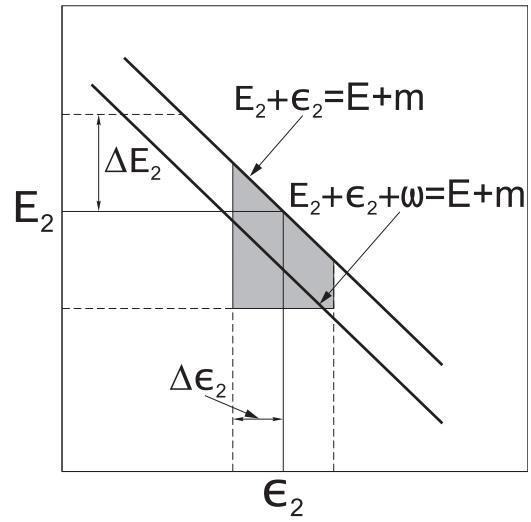

FIG. 3. Plane of the E_2 and ϵ_2 variables where the shaded area represents the kinematically allowed region within the experimental setup.

limited. In our calculation we restrict ourselves with the region $\epsilon_2 < \epsilon_{2\max} - \Delta E$, where $\Delta E = \Delta E_2 + \Delta\epsilon_2$ and $\epsilon_{2\max}$ is defined by Eq. (5). In this case we get for the experimental restriction the isotropic condition

$$\omega \leqslant \Delta E.$$

In the other case, $\epsilon_2 > \epsilon_{2\max} - \Delta E$, the restriction for the photon energy is

$$\omega \leqslant \epsilon_{2\max} - \epsilon_2.$$

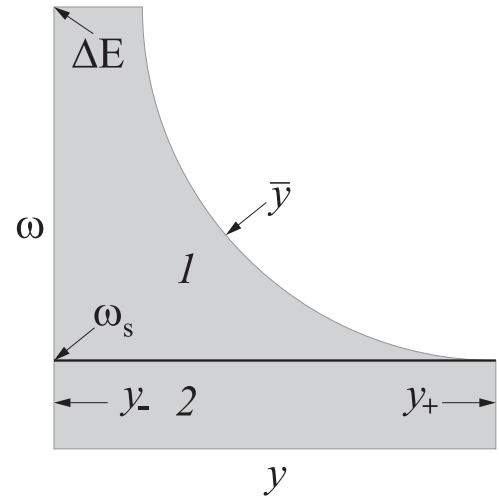

FIG. 4. Integration region over the variables ω and y. Here $y_\pm = E \pm p, \bar{y} = [(m-\epsilon_2)(E-\epsilon_2-\omega) + \sqrt{\epsilon_2^2 - m^2}\sqrt{(E+m-\epsilon_2-\omega)^2 - M^2}]/\omega$. The quantity ω_s is defined by positive solution of the equation $\bar{y} = y_+$ and given by Eq. (45).

In the chosen coordinate system the element of solid angle becomes $d^3k \to 2\pi\,\omega^2\,d\omega\,d\cos\phi$. Now we introduce a new variable $y = E - p\cos\phi > 0$ and rewrite Eq. (43) as

$$\frac{d\sigma^{(h)}}{d\epsilon_2} = \frac{\alpha^3}{16\pi}\frac{1}{mp^2}\int \omega\,d\omega \int d\,y \int_0^{2\pi} \frac{1}{q_1^4\,|\vec{p}-\vec{k}|}\left[-W_1\left(q_1^2\right)S_1 + \frac{W_2\left(q_1^2\right)}{M^2}\,S_2\right]d\,\varphi\,, \tag{44}$$

where the integration region over the variables ω and y is shown in Fig. 4, and

$$\omega_s = (|\vec{k}_2| - |\vec{p}| + x)\frac{M^2|\vec{k}_2|(|\vec{k}_2| + |\vec{p}|) + (m-\epsilon_2)[M^2(x-m) + 2m(2Ex + m^2 - m\epsilon_2)]}{4(m-\epsilon_2)[x(M^2 + m^2 + 2mE) - m(M^2 + mE)] + M^4}, \tag{45}$$

where $x = E + m - \epsilon_2$. The quantity ω_s represents the maximal energy, when the photon can be emitted in the whole angular phase space. The dependence of this quantity on the recoil electron energy, at different values of the proton beam energy, is shown in Fig. 5. We see that it is of the order of the electron mass m in a wide range of the energies ϵ_2 and E. Because our analytical calculations for the soft photon correction were performed under the condition $\bar{\omega} \ll m$, where $\bar{\omega}$ is the maximal energy of the soft photon, we cannot identify ω_s with $\bar{\omega} \ll m$, as it has been done in Ref. [39].

Following the Ref. [39], we include in the integral (44) the weight function $g(\omega)$ given by

$$g(\omega) = 1 \quad \text{for} \quad \bar{\omega} < \omega < \Delta E_2 - \Delta\epsilon_2,$$

$$g(\omega) = \frac{\Delta E_2 + \Delta\epsilon_2 - \omega}{2\Delta\epsilon_2} \quad \text{for} \quad \Delta E_2 - \Delta\epsilon_2 < \omega < \Delta E_2 + \Delta\epsilon_2\,.$$

In fact, the function $g(\omega)$ is the ratio of the straight line segments cut by the lines $E_2 + \epsilon_2 + \omega = E + m$ and $E_2 + \epsilon_2 = E + m$ in the shaded region in Fig. 3.

So, the expression for the cross section given by Eq. (44) can be written as a sum of two terms,

$$\frac{d\sigma^{(h)}}{d\epsilon_2} = \frac{\alpha^3}{16\pi}\frac{1}{m\,p^2}\left[\int_{\omega_s}^{\Delta E} g(\omega)\,C_1(\omega)\,d\omega + \int_{\bar{\omega}}^{\omega_s} C_2(\omega)\,d\omega\right], \tag{46}$$

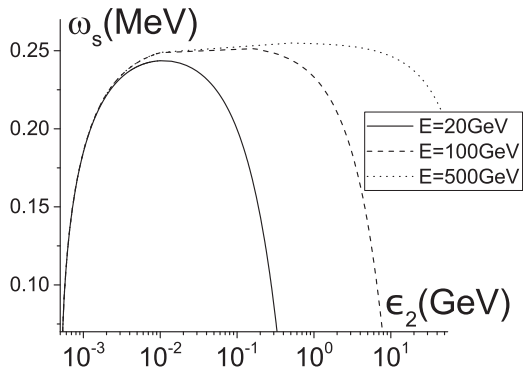

FIG. 5. Maximum energy of the photon when emitted in the whole angular phase space.

where

$$C_1(\omega) = \int_{y_-}^{\bar{y}}\int_0^{2\pi}\left\{\frac{\omega}{q_1^4\,|\vec{p}-\vec{k}|}\left[-W_1\left(q_1^2\right)S_1 + \frac{W_2\left(q_1^2\right)}{M^2}\,S_2\right]\right\} \times d\varphi dy,$$

$$C_2(\omega) = \int_{y_-}^{y_+}\int_0^{2\pi}\left\{\frac{\omega}{q_1^4\,|\vec{p}-\vec{k}|}\left[-W_1\left(q_1^2\right)S_1 + \frac{W_2\left(q_1^2\right)}{M^2}\,S_2\right]\right\} \times d\varphi dy. \tag{47}$$

The scalar products of various four-momenta, which enter in the expressions for S_1, S_2, and q_1^2, are expressed, in terms of the angles, as illustrated in Fig. 2, and the photon energy, as follows:

$$\begin{aligned} d_1 &= -2m\,\omega\,,\ k_1\cdot k_2 = m\,\epsilon_2\,,\ k_1\cdot p_1 = m\,E\,,\\ k\cdot p_1 &= \omega(E - p\cos\phi)\,,\\ d_2 &= 2\,\omega\{\epsilon_2 - |\vec{k}_2|[\cos\theta\,\cos(\eta+\phi)\\ &\quad + \cos\varphi\sin\theta\,\sin(\eta+\phi)]\}\,,\\ k_2\cdot p_1 &= \epsilon_2\,E - p|\vec{k}_2|(\cos\eta\cos\theta + \cos\varphi\sin\eta\sin\theta)\,. \end{aligned} \tag{48}$$

In turn, the respective trigonometric functions of angles are expressed through the photon energy and the variable y, as:

$$\begin{aligned} \cos\eta &= \frac{p^2 - \omega(E-y)}{p|\vec{p}-\vec{k}|}\,,\quad \cos(\eta+\phi) = \frac{E-\omega-y}{|\vec{p}-\vec{k}|}\,,\\ \cos\theta &= \frac{(\epsilon_2 - m)(E+m) + \omega(y+m-\epsilon_2)}{|\vec{p}-\vec{k}|}\,,\\ &\sin\theta\,,\ \sin\eta\,,\ \sin(\eta+\phi) \geqslant 0\,,\\ |\vec{p}-\vec{k}| &= \sqrt{p^2 + \omega(2y - 2E + \omega)}\,. \end{aligned} \tag{49}$$

The functions W_1 and W_2 depend on the azimuthal angle φ, and, in order to perform the integration over this variable in the right-hand side of Eq. (46), one needs to use a specific expressions for the form factors entering these functions. Further, we concentrate on small values of the squared momentum transfer as compared with the proton mass, where the form factors can be expanded in a series in term of powers of q_1^2. In the calculations we keep the terms of the order of 1 , q_1^2, and q_1^4 in the quantity

$$-W_1\left(q_1^2\right)S_1 + \frac{W_2\left(q_1^2\right)}{M^2}\,S_2,$$

which enters the differential cross section.

The integration in the right-hand side of Eq. (46) over the φ and y variables is performed analytically. The result for both $C_1(\omega)$ and $C_2(\omega)$ is very cumbersome, and it was published in the Appendix of our preprint [46]. In the limit $\omega \to 0$ the function $C_1(\omega)$ is regular, and the function $C_2(\omega)$ has an infrared behavior. We extract the regular part $C_{2R}(\omega)$ and the infrared contribution $C_{2I}(\omega)$ by a simple subtraction procedure by writing

$$\begin{aligned} C_2(\omega) &= \big[C_2(\omega) - C_2(\omega \to 0)\big] + C_2(\omega \to 0) \\ &= C_{2R}(\omega) + C_{2I}(\omega)\,, \\ C_{2I}(\omega) &\sim \frac{1}{\omega}\left[\frac{\epsilon_2}{k_2}\ln\frac{\epsilon_2 + k_2}{m} - 1\right]. \end{aligned} \tag{50}$$

The infrared contribution is combined with the correction due to soft and virtual photon emission and this results in changing $\bar{\omega} \to \omega_s$ in the expression for δ_0 [see Eq. (35)]. The integration of the regular part $C_{2R}(\omega)$ over ω (as the lower limit we can chose an arbitrary small value) as well the whole contribution of the region 1, $C_1(\omega)$, is performed numerically.

IV. NUMERICAL ESTIMATIONS AND DISCUSSION

In the following section, the conditions for the experimental uncertainties are set to $\Delta E_2 = 0.02E$ and $\Delta\epsilon_2 = 0.03\epsilon_2$ if other choice is not specified.

Since the four-momentum transfer squared is very small in this reaction, the proton charge and magnetic form factors are approximated by Taylor series expansions. We use the expansion over the variable q^2 of three form-factor parametrizations.

By means of the radii [labeled as (r)]. In this approach, we use the expansion taking into account only the mean-square radii that are determined from Ref. [47]. These radii have been obtained as a result of a comprehensive analysis of the electron-proton scattering data (high statistics Mainz data set) using model-independent constraints from the form factor analyticity. The expansion is defined as follows:

$$\frac{G_{E,M}(q^2)}{G_{E,M}(0)} = 1 + \frac{1}{6}q^2 r_{E,M}^2 + O(q^4), \tag{51}$$

where $r_{E,M}$ is proton electromagnetic charge (magnetic) radius and their values are [47] $r_E = 0.904(15)$ fm $= 4.58$ GeV^{-1}, $r_M = 0.851(26)$ fm $= 4.32$ GeV^{-1}. Thus, electric and magnetic form factors are (q^2 in GeV^{-2}):

$$G_E = 1 + 3.496q^2,\; G_M = 2.793 + 8.65q^2.$$

The dipole fits. In this approach, we use two different dipole fits. The well-known standard one, labeled as (sd), uses both the small- and large-Q^2 data,

$$G_E(q^2) = G,\; G_M(q^2) = \mu_p G,\; G = (1 - 1.41q^2)^{-2}\,, \tag{52}$$

and leads to the following expansions of the form factors, up to the terms q^4,

$$\begin{aligned} G_E &= 1 + 2.82q^2 + 5.96q^4, \\ G_M &= 2.793 + 7.88q^2 + 16.65q^4. \end{aligned}$$

TABLE I. Parameters for the proton form factor fits in Eq. (54) used in this work, with n_i, m_i, d_i, and g_i in units of GeV^2.

n_1	0.38676	m_1	1.01650
n_2	0.53222	m_2	− 19.0246
d_1	3.29899	g_1	0.40886
d_2	0.45614	g_2	2.94311
d_3	3.32682	g_3	3.12550

Another dipole fit [48], labeled as (d), uses only the lower-Q^2 data by MAMI Collaboration

$$G_E(q^2) = (1 - 1.517\,q^2)^{-2},\; G_M(q^2) = \mu_p(1 - 1.37q^2)^{-2}\,, \tag{53}$$

and gives

$$\begin{aligned} G_E &= 1 + 3.034q^2 + 6.91q^4, \\ G_M &= 2.793 + 7.65q^2 + 15.72q^4. \end{aligned}$$

The sum of monopole terms [labeled as (m)]. In this approach, we use the five-parameter fit for both Dirac and Pauli form factors as a sum of three monopoles [49],

$$F_1(q^2) = \sum_1^3 \frac{n_i}{d_i - q^2},\; F_2(q^2) = \sum_1^3 \frac{m_i}{g_i - q^2}, \tag{54}$$

where n_i, m_i, d_i and g_i are free parameters, and the parameters n_3 and m_3 are determined from the normalization conditions

$$F_1(0) = \sum_i \frac{n_i}{d_i},\; F_2(0) = \sum_i \frac{m_i}{g_i}.$$

The parameters n_i,m_i,d_i, and g_i for the F_1 and F_2 proton form factors are given in Table I. The normalization conditions are $F_1(0) = 1$ and $F_2(0) = \mu_p - 1$, where $\mu_p = 2.793$ is the proton total magnetic moment.

Thus, we have for the parameters n_3 and m_3

$$\begin{aligned} n_3 &= d_3 - d_3\left(\frac{n_1}{d_1} + \frac{n_2}{d_2}\right), \\ m_3 &= g_3(\mu_p - 1) - g_3\left(\frac{m_1}{g_1} + \frac{m_2}{g_2}\right). \end{aligned}$$

The expansions for the form factors $G_{E,M}$ are

$$\begin{aligned} G_E &= 1 + \left[\sum \frac{n_i}{d_i^2} + \frac{\mu_p - 1}{4M^2}\right]q^2 \\ &\quad + \left[\sum \frac{n_i}{d_i^3} + \frac{1}{4M^2}\sum \frac{m_i}{g_i^2}\right]q^4\,, \\ G_M &= \mu_p + \left[\sum \frac{n_i}{d_i^2} + \sum \frac{m_i}{g_i^2}\right]q^2 \\ &\quad + \left[\sum \frac{n_i}{d_i^3} + \sum \frac{m_i}{g_i^3}\right]q^4\,. \end{aligned} \tag{55}$$

The expansion of the form factors is as follows:

$$\begin{aligned} G_E &= 1 + 3.017\,q^2 + 7.22\,q^4\,, \\ G_M &= 2.793 + 8.239\,q^2 + 20.31\,q^4\,. \end{aligned}$$

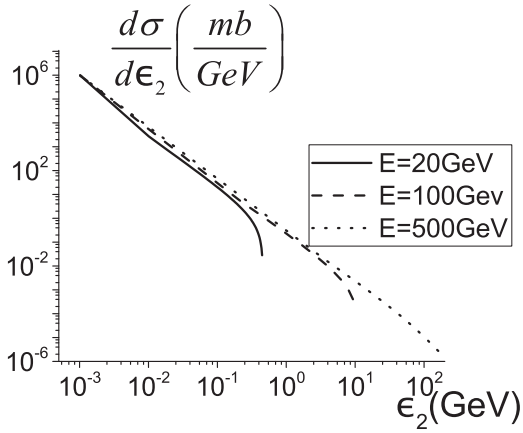

FIG. 6. Born differential cross section, defined by Eq. (13), is calculated with the standard dipole fit of the form factors at different beam energies.

The d- and m-parameterizations give very close distributions, and therefore, we use only m-parametrization in our numerical calculations.

One-parameter linear model in conformal mapping variable [labeled as (z)]. This approach is to use an expansion in q^2 of the approximation to the form factors given by one-parameter formulas,

$$G_E^2 = 1 - C_E\, z\,,\ \ G_M^2 = \mu_p^2(1 - C_M\, z)\,,$$
$$z = \frac{\sqrt{4m_\pi^2 - q^2} - \sqrt{4m_\pi^2}}{\sqrt{4m_\pi^2 - q^2} + \sqrt{4m_\pi^2}}\,, \tag{56}$$

with [48],

$$C_E = 2.105\,,\ \ C_M = 2.04\,.$$

In this case, the expansion for the form factors reads

$$G_E = 1 + 3.018\, q^2 + 7.221\, q^4\,,$$
$$G_M = 2.793 + 9.133\, q^2 + 43.65\, q^4\,.$$

To understand better the small-Q^2 distribution and its dependence on r_E^2, we expand the parametrizations of the function $\mathcal{D}$ defined by Eq. (14) for radii (r) (when the electric form factor is smallest) and monopole (when the electric form factor is middle) at two values of the proton beam energy: 100 and 500 GeV

$$\mathcal{D}(r, E = 100\ \text{GeV}) = 0.0209 + \left(1.92 + 0.00582\, r_E^2\right)q^2 + \left(3.71 + 0.657\, r_E^2 + 0.00058\, r_E^4\right)q^4\,,$$
$$\mathcal{D}(m, E = 100\ \text{GeV}) = 0.0209 + \left(1.92 + 0.00696\, r_E^2\right)q^2 + \left(3.74 + 0.657\, r_E^2 + 0.00145\, r_E^4\right)q^4\,,$$
$$\mathcal{D}(r, E = 500\ \text{GeV}) = 0.5222 + \left(1.772 + 0.174\, r_E^2\right)q^2 + \left(-5.031 + 0.977 r_E^2 + 0.014\, r_E^4\right)q^4\,,$$
$$\mathcal{D}(m, E = 500\ \text{GeV}) = 0.5222 + \left(1.772 + 0.174\, r_E^2\right)q^2 + \left(-4.203 + 0.977 r_E^2 + 0.036\, r_E^4\right)q^4\,, \tag{57}$$

where r_E^2 must be taken in GeV^{-2}.

There is a compensation of the first two terms of these expansions when $|q^2|$ increases, and since the coefficient in front of q^4 is large, it has to be taken into account even at small-enough values of $|q^2|$. The coefficient in front of r_E^2 in the second term increases rapidly with the growth of the beam energy.

To illustrate the dependence of the recoil electron distribution on the proton beam energy, the Born cross section is shown in Fig. 6 for the standard dipole fit at $E = 20$ GeV, 100 GeV, and 500 GeV. Here and further for the beam energy 500 GeV we restrict the recoil electron energy by 50 GeV, because for larger values the above expansions of the form factors are incorrect.

The sensitivity of this cross section to different form-factor parametrizations is shown in Fig. 7, in terms of the quantities (in percentages)

$$R^r = 1 - \frac{d\,\sigma^r}{d\,\sigma^{sd}}\,,\ \ R^m = 1 - \frac{d\,\sigma^m}{d\,\sigma^{sd}}\,,\ \ R^z = 1 - \frac{d\,\sigma^z}{d\,\sigma^{sd}}\,, \tag{58}$$

where $d\,\sigma^i$ is the differential cross section (13), and the indices $i = r\,, z\,, m\,, d$ correspond to the above-mentioned parametrizations of the proton form factors.

The hard photon correction depends on the parameters ΔE_2 and $\Delta\epsilon_2$, due to the contribution of the region 1 in Fig. 4. To illustrate this dependence, we show in Fig. 8 the quantities (in

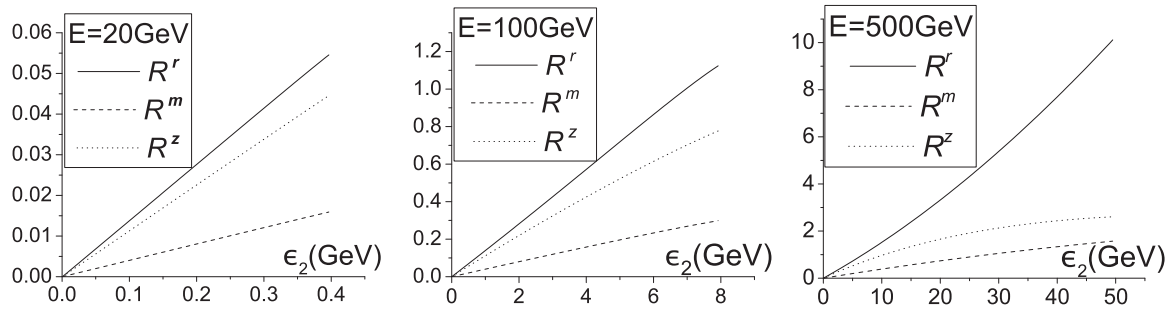

FIG. 7. The difference of the recoil electron distributions [Eq. (58)] in percentages for various parametrizations of the form factors at proton energies 20 GeV, 100 GeV, and 500 GeV.

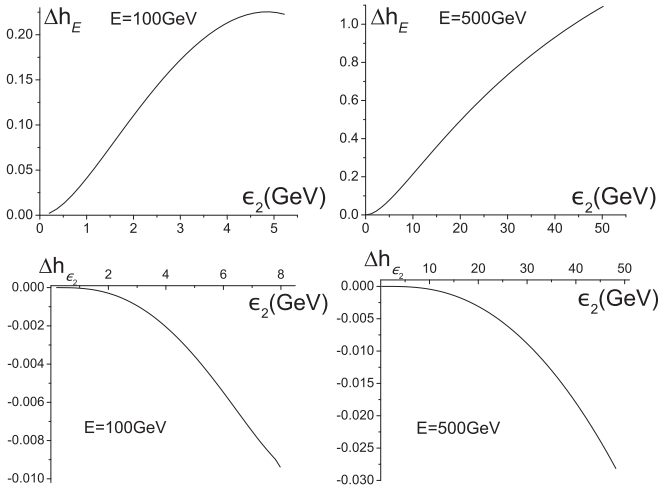

FIG. 8. The sensitivity, as the function of the recoil electron energy (in percentage) of the hard photon correction to the parameter ΔE_2 (above) and $\Delta\epsilon_2$ (bottom) Eq. (59) at proton energy of 100 GeV (left) and 500 GeV (right).

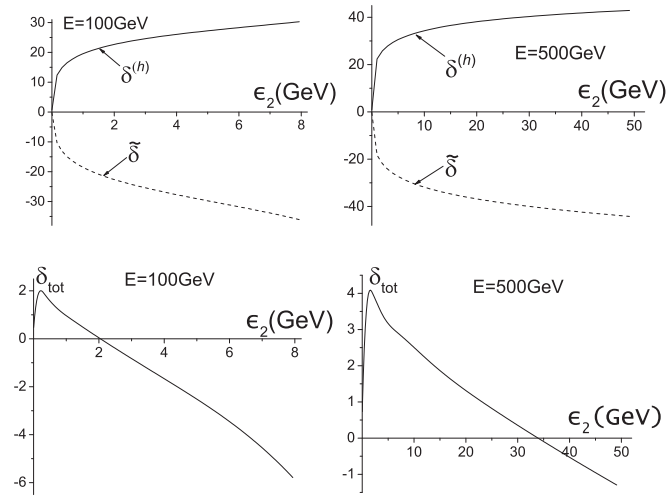

FIG. 9. (Top) The modified soft and virtual ($\widetilde{\delta}$) (dashed line) and hard [$\delta^{(h)}$] (solid line) corrections (in percentage) as defined by Eq. (61). (Bottom) The total radiative correction (in percentage) calculated for the standard dipole fit at $\Delta E_2 = 0.02\,E$, at 100 GeV (left) and 500 GeV (right) incident proton energy.

which the contribution of the region 2 is removed)

$$\Delta h_E = \frac{d\,\sigma^{(h)}(\Delta E_2 = 0.05\,E\,, \Delta\epsilon_2 = 0.03\,\epsilon_2)}{d\,\sigma^{(B)}} - \frac{d\,\sigma^{(h)}(\Delta E_2 = 0.02\,E\,, \Delta\epsilon_2 = 0.03\,\epsilon_2)}{d\,\sigma^{(B)}},$$
$$\Delta h_\epsilon = \frac{d\,\sigma^{(h)}(\Delta E_2 = 0.02\,E\,, \Delta\epsilon_2 = 0.06\,\epsilon_2)}{d\,\sigma^{(B)}} - \frac{d\,\sigma^{(h)}(\Delta E_2 = 0.02\,E\,, \Delta\epsilon_2 = 0.03\,\epsilon_2)}{d\,\sigma^{(B)}}, \quad (59)$$

as a function of the recoil electron energy for the *sd* parametrization. The cross section increases with the growth of ΔE_2 at fixed value $\Delta\epsilon_2$ but even decreases with the growth of $\Delta\epsilon_2$ at fixed ΔE_2. Such unusual dependence on the energy-cut parameters is due to the weight function $g(\omega)$ in the integrand over the region 1 in Fig. 4. If ΔE_2 increases, then the region where $g(\omega) = 1$ is enlarged. Meanwhile, the region where $g(\omega) < 1$ is only shifted but the function $g(\omega)$ grows, and these effects lead to the enhancement of the cross section. With the increase of $\Delta\epsilon_2$ the region where $g(\omega) = 1$ is reduced, and the region where $g(\omega) < 1$ is enlarged and $g(\omega)$ decreases. The change of the cross section in the last case depends on interplay of these factors as well as on the integrand.

Qualitatively, it can be understood if we replace $C_1(\omega)$ in the right-hand side of Eq. (46) by its small-ω behavior $\sim 1/\omega$ and perform analytical integration,

$$\int_{\omega_s}^{\Delta E} g(\omega)\,\frac{d\omega}{\omega} = \ln\frac{\Delta E_2}{\omega_s} - \frac{1}{6}\left(\frac{\Delta\epsilon_2}{\Delta E_2}\right)^2, \quad \frac{\Delta\epsilon_2}{\Delta E_2} \ll 1. \quad (60)$$

Thus, when parameters ΔE_2 and $\Delta\epsilon_2$ grow, the logarithmic increase with ΔE_2 and a very weak decrease with $\Delta\epsilon_2$ take place.

Note that our choice of parameters ΔE_2 and $\Delta\epsilon_2$ is taken only for illustration. Really, they have to be specific for every experiment, but our approach allows us to calculate with any ones.

In Fig. 9 we present the quantities $\delta^{(h)}$ and $\widetilde{\delta}$, defined as

$$\delta^{(h)} = \frac{d\,\sigma^{(h)}}{d\,\sigma^{(B)}} - \frac{2\,\alpha}{\pi}\ln\frac{\omega_s}{\bar\omega}\left[\frac{\epsilon_2}{k_2}\ln\left(\frac{\epsilon_2 + k_2}{m}\right) - 1\right],$$
$$\widetilde{\delta} = \bar\delta + \delta^{(\mathrm{vac})} + \frac{2\,\alpha}{\pi}\ln\frac{\omega_s}{m}\left[\frac{\epsilon_2}{k_2}\ln\left(\frac{\epsilon_2 + k_2}{m}\right) - 1\right], \quad (61)$$

which we call "modified hard and soft and virtual corrections," respectively, as well as their sum $\delta_{\mathrm{tot}} = \delta^{(h)} + \widetilde{\delta}$ that is the total model-independent first-order radiative correction [the last term in $\bar\delta$ is $\delta_0(\bar\omega \to \omega_s)$]. In fact,

$$\delta_{\mathrm{tot}} = \delta^{(h)} + \bar\delta = \delta_0 + \bar\delta + \delta^{(\mathrm{vac})} + \frac{d\sigma^{(h)}}{d\sigma^{(B)}}.$$

Note that both modified corrections in Eq. (61) are independent on the auxiliary parameter $\bar\omega$ but depend on the physical parameter ω_s and, therefore, have a physical sense.

To calculate σ_{tot}, we can write the quantity $[1 + \delta_0(\bar\omega \to \omega_s)]$ using the expression (35) or its exponential form defined by (36) (with substitution $\bar\omega \to \omega_s$). But numerical estimations show that they differ very insignificantly, by a few tenths of a percentage, and, further, we do not use the exponential form.

We see that at small values of the squared momentum transfer (small recoil-electron energy ϵ_2) the total model-independent radiative correction is positive and it decreases (with increase of ϵ_2), reaching zero and becoming negative. The absolute value of the radiative correction does not exceed 6%, although the strong compensation of the large (up to 40%) positive "modified hard" and negative "modified soft and virtual" corrections takes place. Such behavior of the pure QED correction is similar to one derived in Ref. [39].

If the proton form factors are determined independently with high accuracy from other experiments, the measurement of the cross section $d\,\sigma/d\,\epsilon_2$ can be used, in principle, to

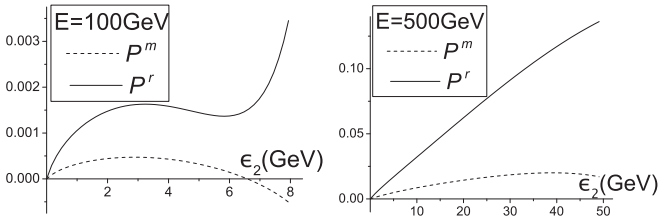

FIG. 10. The sensitivity of the total model-independent radiative correction (in percentage) to the choice of the form-factor parametrization [Eq. (62)].

measure the model-dependent part of the radiative correction in the considered conditions. This possibility is similar to the one described in Ref. [43] where the authors proposed to determine the hadronic (model-dependent) contribution to the running electromagnetic coupling $\alpha(q^2)$ by a precise measurement of the $\mu^- - e^-$ differential cross section, assuming that QED model-independent radiative corrections are under control.

In Fig. 10 we illustrate the sensitivity of the total radiative correction to the parametrization of the form factors in terms of the ratios

$$P^i = \frac{1+\delta^i_{\rm tot}}{1+\delta_{\rm tot}} - 1\,, \quad i = r, m\,, \tag{62}$$

where $\delta_{\rm tot}$ is the total correction for standard dipole fit. We see that, in the considered conditions, the deviation of these quantities from unity is very small and conclude that the influence of the parametrizations of the form factors on the radiative correction is much smaller than this influence on the Born cross section. Moreover, the r and m parametrizations decrease the Born cross section relative to the d one, as it follows from Fig. 7, whereas for the radiative correction we have just the opposite effect.

V. CONCLUSION

In present paper we investigated the recoil-electron energy distribution in elastic proton-electron scattering in coincidence experimental setup, taking the model-independent QED radiative corrections into account. The detection of the recoil electron in this process, with energies from a few MeV up to a few tens of GeV, will allow us to receive the small-Q^2 data, at $10^{-5}\,{\rm GeV}^2 \leqslant Q^2 \leqslant 3\times10^{-2}\,{\rm GeV}^2$. Such data, being combined with the existing experiments and planned future experiments with the electron beams, will help to perform more precise analysis of the small-Q^2 behavior of the proton electromagnetic form factors. It allows us to obtain meaningful extrapolation to the static point and to extract the proton charge radius. As noted in the recent review [50], it is interesting to extract the proton charge radius entirely from low-Q^2 data. High-precision measurements, in the inverse kinematics, allow us to accumulate a lot of such data.

To cover the above-mentioned interval of the Q^2 values, it is desirable to use the proton beams with large-enough energies of the order of a few hundred GeV. At very small Q^2, the sensitivity of the differential cross section to the form-factor parametrizations is practically absent, but at $Q^2 \approx 2\times10^{-3}\,{\rm GeV}^2$ it has become noticeable and reaches several percentages at $Q^2 \approx 3\times10^{-2}\,{\rm GeV}^2$ (see Fig. 7). As follows from the relations (57), the sensitivity to the value of the proton charge radius also increases essentially with the growth of the proton beam energy.

The effect, caused by the changing of the form-factor parametrization in the small-Q^2 region, is rather small. Therefore, the accuracy of the measurement has to be high enough. In Ref. [32], it is noted that in planning an experiment at the Mainz Microtron, with detection of the recoil proton, the measurement precision has to be at the level of 0.2%. To discriminate between different form-factor parametrizations, the accuracy, in the inverse kinematics experiments, must be the same, possibly somewhat less with growth of Q^2 and the proton beam energy. At such conditions, the radiative corrections have to be under control.

We account for the first-order QED corrections caused by the vacuum polarization and the radiation of the real and virtual photons by the initial and final electrons, paying special attention to the calculation of the hard photon emission contribution when the final proton and electron energies are determined. This hard radiation takes place due to the imprecision in the measurement of the proton (electron) energy, ΔE_2 ($\Delta\varepsilon_2$). In our calculations, we follow Ref. [39] in choosing the coordinate system and the angular integration method. We derive analytical (although very cumbersome) expressions for the functions $C_1(\omega)$ and $C_2(\omega)$, defined by Eqs. (47). The cancelation of the auxiliary infrared parameter $\bar\omega$ in the sum of the soft and hard corrections is performed analytically and the remaining ω integration in (46) is done numerically.

The increase of the parameter $\Delta\epsilon_2$ leads to the small decrease of the hard photon correction. The magnitude of this decrease is about 0.01 (0.025)% at $E = 100$ (500) GeV. In contrast, the increase of the parameter ΔE_2 increases the hard photon correction by ≈ 0.2 (1)% at $E = 100$ (500) GeV (see Fig. 8). Such different behavior of this correction can be explained, on the qualitative level, by Eq. (60).

As usual, there is a strong cancellation between the positive hard correction and negative virtual and soft ones, as seen in Fig. 9. Despite the fact that the absolute values of these corrections separately reach 20–40%, their sum $|\delta_{\rm tot}|$ does not exceed 6% at $E = 100$ GeV and 4% at $E = 500$ GeV for the values $\Delta E_2 = 0.02\,E$, $\Delta\varepsilon_2 = 0.3\,\varepsilon_2$ used in calculations. The total correction shows the very weak dependence on the form-factor parametrization (see Fig. 10) in the considered region. At the lower values of Q^2, which correspond to the lower values of the recoil electron energy ε_2, the total correction $\delta_{\rm tot}$ is positive and changes sign when Q^2 increases. Such behavior of $\delta_{\rm tot}$ is similar to the one found in Ref. [39] and confirmed in Ref. [40] for the case of the pion electron scattering.

In Refs. [39,40], the authors calculated also the model-dependent part of the radiative corrections, using the pointlike scalar electrodynamics to describe the interaction of the charged pion with a photon.

In our case, the effect of the model-dependent corrections, when virtual and real photons are emitted by the initial and final protons, can be roughly evaluated in the approximation of the structureless proton with the minimal proton-photon

interaction $[F_1(q^2) = 1\,,\ F_2(q^2) = 0]$ under the condition $Q^2/M^2 \ll 1$. The account for the proton structure cannot change estimation essentially. To derive the virtual and soft corrections in this approximation, it is enough to write, in the expression $(\delta_0 + \bar{\delta})$ defined in Eq. (35) (where $\bar{\delta}$ is taken without the term proportional to M^2), ε_2 and k_2 in terms of Q^2 and m and after that to change $m \to M$ and then to use the condition $Q^2/M^2 \ll 1$. Such a procedure gives their sum as

$$\frac{\alpha}{\pi}\frac{Q^2}{M^2}\left(\frac{85}{36} + \frac{4}{3}\ln\frac{M^2}{Q^2} + \frac{2}{3}\ln\frac{\bar{\omega}}{M} - 2\ln 2\right). \qquad (63)$$

The largest negative term with the unphysical parameter $\bar{\omega}$ has to be canceled by the hard photon contribution. The remaining terms, in (63) at $Q^2 = 3 \times 10^{-2}\,\mathrm{GeV}^2$, do not exceed 0.5×10^{-3}, which is a few times smaller than the required measurement accuracy. In this approximation, the vertex correction modifies also the Born value of the proton anomalous magnetic moment and that leads to

$$G_M(q^2) \to G_M(q^2) + \frac{\alpha}{2\pi}\left(1 + \frac{q^2}{6M^2}\right).$$

Taking $\mu_p = 2.793$, we evaluate that the correction to the Born value of G_M^2 is no more than 0.8×10^{-3}. The up-down interference, that is, part of the model-dependent QED corrections, which include the two-photon exchange and the interference of the proton and electron radiation, has to be suppressed in the considered kinematics at least by the factor

$$\frac{\alpha}{\pi}\frac{Q^2}{2m\,E}\ln\frac{2m\,E}{Q^2},$$

that is, by no more than 0.1%. The analysis of the two-photon-exchange in the elastic $e^- - p$ scattering at small-Q^2, performed in Ref. [51] in frame of a model, confirms such suppression.

Thus, we conclude that the model-independent radiative corrections are under control and, if necessary, can be calculated with higher accuracy. We believe that the uncertainty due to the model-dependent part in the region $Q^2 \ll M^2$ is small and cannot affect the experimental cross sections measured even with 0.2% accuracy.

ACKNOWLEDGMENTS

This work was partially supported by the Ministry of Education and Science of Ukraine (Projects No. 0115U000474 and No. 0117U004866). The research was conducted in the scope of the IDEATE International Associated Laboratory (LIA).

[1] S. Pacetti, R. Baldini Ferroli, and E. Tomasi-Gustafsson, Phys. Rep. **550-551**, 1 (2015).
[2] A. I. Akhiezer and M. P. Rekalo, Sov. Phys. Dokl. **13**, 572 (1968) [Dokl. Akad. Nauk Ser. Fiz. **180**, 1081 (1968)].
[3] A. I. Akhiezer and M. P. Rekalo, Sov. J. Part. Nucl. **4**, 277 (1974) [Fiz. Elem. Chast. Atom. Yadra **4**, 662 (1973)].
[4] A. Puckett, E. Brash, M. Jones, W. Luo, M. Meziane *et al.*, Phys. Rev. Lett. **104**, 242301 (2010).
[5] E. A. Kuraev, Y. M. Bystritskiy, A. I. Ahmadov, and E. Tomasi-Gustafsson, Phys. Rev. C **89**, 065207 (2014).
[6] A. V. Gramolin and D. M. Nikolenko, Phys. Rev. C **93**, 055201 (2016).
[7] J. Arrington, Phys. Rev. C **69**, 032201 (2004).
[8] E. Tomasi-Gustafsson, Phys. Part. Nucl. Lett. **4**, 281 (2007).
[9] S. Pacetti and E. Tomasi-Gustafsson, Phys. Rev. C **94**, 055202 (2016).
[10] C. Perdrisat, V. Punjabi, and M. Vanderhaeghen, Prog. Part. Nucl. Phys. **59**, 694 (2007).
[11] R. Pohl, A. Antognini, F. Nez, F. D. Amaro, F. Biraben *et al.*, Nature **466**, 213 (2010).
[12] A. Antognini *et al.*, Science **339**, 417 (2013).
[13] P. J. Mohr, D. B. Newell, and B. N. Taylor, Rev. Mod. Phys. **88**, 035009 (2016).
[14] X. Zhan *et al.*, Phys. Lett. B **705**, 59 (2011).
[15] J. C. Bernauer *et al.* (A1 Collaboration), Phys. Rev. Lett. **105**, 242001 (2010).
[16] A. Antognini *et al.*, J. Phys. Conf. Ser. **312**, 032002 (2011).
[17] D. Tucker-Smith and I. Yavin, Phys. Rev. D **83**, 101702 (2011).
[18] B. Batell, D. McKeen, and M. Pospelov, Phys. Rev. Lett. **107**, 011803 (2011).
[19] M. M. Giannini and E. Santopinto, (2013) arXiv:1311.0319 [hep-ph].
[20] E. Kraus, K. E. Mesick, A. White, R. Gilman, and S. Strauch, Phys. Rev. C **90**, 045206 (2014).
[21] I. Lorenz, H.-W. Hammer, and U.-G. Meissner, Eur. Phys. J. A **48**, 151 (2012).
[22] I. T. Lorenz, Ulf-G. Meißner, H.-W. Hammer, and Y.-B. Dong, Phys. Rev. D **91**, 014023 (2015).
[23] M. Horbatsch, E. A. Hessels, and A. Pineda, Phys. Rev. C **95**, 035203 (2017).
[24] C. Peset and A. Pineda, Nucl. Phys. B **887**, 69 (2014).
[25] K. Griffioen, C. Carlson, and S. Maddox, Phys. Rev. C **93**, 065207 (2016).
[26] M. O. Distler, T. Walcher, and J. C. Bernauer, (2015) arXiv:1511.00479 [nucl-ex].
[27] J. C. Bernauer and M. O. Distler, (2016) arXiv:1606.02159 [nucl-th].
[28] J. C. Bernauer, (2014) arXiv:1411.3743 [nucl-ex].
[29] A. Gasparian (PRad at JLab), Eur. Phys. J. Web Conf. **73**, 07006 (2014).
[30] E. J. Downie, Eur. Phys. J. Web Conf. **113**, 05021 (2016).
[31] D. Marchand (PRAE Collaboration) Eur. Phys. J Web Conf. **138**, 01012 (2017).
[32] A. Vorobyev, in *7th Workshop on Hadron Structure and QCD: From Low to High Energies* (2016).
[33] G. Gakh, A. Dbeyssi, E. Tomasi-Gustafsson, D. Marchand, and V. Bytev, Phys. Part. Nucl. Lett. **10**, 393 (2013).
[34] G. I. Gakh, A. Dbeyssi, D. Marchand, E. Tomasi-Gustafsson, and V. V. Bytev, Phys. Rev. C **84**, 015212 (2011).
[35] G. Adylov *et al.*, Phys. Lett. B **51**, 402 (1974).
[36] E. B. Dally *et al.*, Phys. Rev. Lett. **39**, 1176 (1977).
[37] E. B. Dally *et al.*, Phys. Rev. Lett. **48**, 375 (1982).
[38] E. B. Dally *et al.*, Phys. Rev. Lett. **45**, 232 (1980).
[39] J. Kahane, Phys. Rev. **135**, B975 (1964).

[40] D. Y. Bardin, V. B. Semikoz, and N. M. Shumeiko, Yad. Fiz. **10**, 1020 (1969).
[41] S. R. Amendolia *et al.* (NA7), Nucl. Phys. B **277**, 168 (1986).
[42] S. R. Amendolia *et al.*, Phys. Lett. B **146**, 116 (1984).
[43] G. Abbiendi *et al.*, Eur. Phys. J. C **77**, 139 (2017).
[44] G. 't Hooft and M. Veltman, Nucl. Phys. B **153**, 365 (1979).
[45] E. A. Kuraev and V. S. Fadin, Sov. J. Nucl. Phys. **41**, 466 (1985) [Yad. Fiz. **41**, 733 (1985)].
[46] G. I. Gakh, M. I. Konchatnij, N. P. Merenkov, and E. Tomasi-Gustafsson, (2016) arXiv:1612.02139 [hep-ph].
[47] G. Lee, J. R. Arrington, and R. J. Hill, Phys. Rev. D **92**, 013013 (2015).
[48] M. Horbatsch and E. A. Hessels, Phys. Rev. C **93**, 015204 (2016).
[49] P. G. Blunden, W. Melnitchouk, and J. A. Tjon, Phys. Rev. C **72**, 034612 (2005).
[50] R. J. Hill, EPJ Web Conf. **137**, 01023 (2017).
[51] M. Gorchtein, Phys. Rev. C **90**, 052201(R) (2014).